Available online at www.sciencedirect.com
SCIENCE DIRECT
Catalysis Today 105 (2005) 436–442
CATALYSIS TODAY
www.elsevier.com/locate/cattod

Lanthanum ferrite membranes in ammonia oxidation Opportunities for 'pocket-sized' nitric acid plants

Javier Pérez-Ramírez [a,*], Bent Vigeland [b]

[a] Yara Technology Centre Porsgrunn, P.O. Box 2560, N-3908 Porsgrunn, Norway
[b] Norsk Hydro, Corporate Research Centre, P.O. Box 2560, N-3908 Porsgrunn, Norway

Available online 12 July 2005

Abstract

This paper reports the application of mixed conducting perovskite membranes for simultaneous in situ O_2 separation and catalytic oxidation of ammonia to nitric oxide. Calcium and strontium-substituted lanthanum ferrite perovskites ($La_{1-x}A_xFeO_{3-\delta}$, with A = Ca, Sr and $x = 0.1$–0.2) were prepared by a conventional wet complexation route with citric acid. Dense membrane disks were obtained by uniaxial pressing of the calcined powders followed by sintering. The oxidation of ammonia over these catalytic membranes in the temperature range of 1000–1333 K leads to NO selectivities up to 98% with no N_2O production, showing stable performance during several days on stream. This novel process demonstrates the great potential for intensification of nitric acid manufacture into miniaturized plants and is considered to be particularly attractive for on-site production of this important bulk chemical.

Keywords: Ammonia oxidation; Reactive separation; Dense membrane; Perovskite; Lanthanum ferrite; Process intensification; Nitric acid production

1. Introduction

Ammonia is oxidized over Pt–Rh alloy gauzes at 1073–1223 K to form NO as the first step in the industrial production of nitric acid, typically originating NO yields of 94–96% and 4–6% of by-products (N_2O and N_2) [1,2]. Major drawbacks associated with the well-established platinum-based catalysts are: (i) high production cost, (ii) metal loss in the form of volatile oxides, and (iii) the production of N_2O, an environmentally harmful gas contributing to the greenhouse effect and ozone depletion. Nitric acid production is the largest single source of N_2O in the chemical industry (125 Mton CO_2-eq. per year), and the development and implementation of abatement technology for this gas is being required [3].

The above aspects have stimulated research for replacing noble metals by oxide catalysts for NH_3 oxidation. Oxides may offer the advantage of lower investment, a simpler manufacture, and a reduced N_2O emission [3,4]. A vast number of patent applications have claimed the promising performance of spinels or perovskites in the reaction, preferably containing cobalt, but also iron, manganese, bismuth, or chromium [4]. Laboratory, pilot, or plant tests have been carried out in fixed-bed reactors using oxides in the form of particles, pellets, or monoliths. Despite extensive research efforts, the industrial implementation of oxides is still prevented by their relatively low NO selectivity as compared to noble metal gauzes and the rapid deactivation under relevant reaction conditions [3]. At most, oxide-based catalysts have been installed right after a reduced number of Pt–Rh gauzes in the ammonia burner, participating to a limited extent in the oxidation of ammonia unconverted by the noble metal catalyst layer. The successful implementation of the so-called dual-stage or hybrid ammonia oxidation reactor in plants is claimed in [4], but does not tackle the real challenge of completely abandoning the utilization of noble metals in the production of nitric acid.

The exploitation of mixed ionic and electronic conductors (MIECs) in a membrane form within the chemical industry is an area of growing interest, since separation and reaction processes can be integrated in a single reactive

* Corresponding author. Present address: Institute of Chemical Research of Catalonia (ICIQ), Av. Països Catalans 16, E-43007 Tarragona, Spain. Fax: +34 977 92 0224.
E-mail address: jperez@iciq.es (J. Pérez-Ramírez).

0920-5861/$ – see front matter © 2005 Elsevier B.V. All rights reserved.
doi:10.1016/j.cattod.2005.06.057

separation unit. Dense ceramic oxygen-ion conducting perovskite membranes are promising systems for oxidation reactions, as air can be used as an oxidant with no mixing of nitrogen with the product stream. This is often a difficult separation and can lead to process cost savings. Besides, reaction selectivity may be improved as gas-phase oxygen is no longer present on the reaction side of the membrane. As recently reviewed by Thursfield and Metcalfe [5], the vast majority of the work with perovskite membranes in disk or tubular configurations has been devoted to high-temperature applications, where appreciable oxygen fluxes are obtained. This includes the partial oxidation of methane to syngas and to a lesser extent the oxidative coupling of methane. The doped lanthanum cobaltite families have attracted great attention with particular interest in the chemically and mechanically robust $La_{0.6}Sr_{0.4}Co_{0.2}Fe_{0.8}O_{3-\delta}$ because of its good ionic and electronic conductivity [5].

This paper introduces a novel process for NH_3 oxidation using lanthanum ferrite-based perovskite membranes, leading to NO selectivities up to 98% and no N_2O formation. We have integrated in a single membrane reactor the separately reported properties of the perovskite materials as oxygen conductors [6] and selective catalysts for ammonia oxidation [7]. As schematically depicted in Fig. 1, the applied configuration combines separation of oxygen from air at the feed side by transport through ionic vacancies in the mixed conducting membrane and reaction of oxygen with ammonia to nitric oxide on the membrane surface at the permeate side. Accordingly, the surfaces of the membrane at the feed and permeate sites function as reduction ($O_2 \rightarrow 2O^{2-}$) and oxidation ($NH_3 \rightarrow NO$) catalysts, respectively. The presented membrane reactor gives rise to a radically intensified process for nitric acid manufacture, being potentially attractive for decentralized production units.

2. Experimental

Lanthanum ferrite-based perovskites ($La_{1-x}A_xFeO_{3-\delta}$, with A = Ca, Sr and $x = 0.1$–0.2) were prepared by a conventional wet complexing route using citric acid. Standardized nitrate solutions (1 M) of the metals were mixed with citric acid in a molar ratio of acid to total cations = 3. The resulting solution was slowly heated to 433 K (40 K h^{-1}) to ensure complete complexation and left overnight at this temperature to dry. The dried samples were heated at 773 K for 5 h in flowing air for the removal of organic matter and finally calcined in static air at 1173 K for 10 h. The resulting powders were characterized by XRF (Bruker AXS S4 Pioneer), XRD (Philips X'Pert), N_2 adsorption at 77 K (Micromeritics TriStar 3000), Hg porosimetry (Carlo Erba 2000), He picnometry (Micromeritics AccuPyc 1330), envelope density analysis (Micromeritics GeoPyc 1360), and laser diffraction (Horiba LS-920). Dense membrane disks (>95% of theoretical density) were made by uniaxial pressing and sintering at 1573 K. After final grinding and polishing, membrane disks with a diameter of 10 mm (ca. 80 mm^2) and a thickness of ca. 0.9 mm were obtained. SEM-EDS analyses of the membrane disks were carried out in a JEOL JSM 5600 LV microscope equipped with a Thermo Vantage detector.

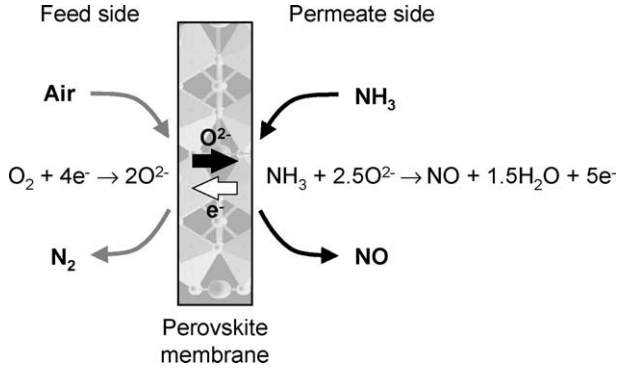

Fig. 1. Reactive separation using mixed conducting membranes: simultaneous in situ O_2 separation from air in the feed side and NH_3 oxidation to NO in the permeate side.

For testing, the membrane disks were mounted in a quartz microreactor, sketched in Fig. 2, which was heated to 1333 K for sealing using gold rings. The oxidation of ammonia was investigated in the temperature range of 1000–1333 K by feeding an equimolar mixture of O_2 + Ar to the feed side and mixtures of NH_3 + He to the permeate side. The inlet ammonia flow was varied in the range of 0.05–4.5 ml NH_3 (STP) min^{-1}, with a total gas flow of 130 ml (STP) min^{-1}. The duration of the tests was typically 10 days, involving periodic repetition of measurements at selected temperature/flow conditions. Product gases were analyzed on-line using a mass spectrometer (Balzers QMG 421C) and a gas microchromatograph (Agilent 3000). The absence of leakages was verified by the absence of Ar at the permeate side. The oxygen flux $J(O_2)$ was determined from the measured concentrations of all the O-containing species. The NO selectivity was determined from the concentrations of the different N-containing products at the reactor outlet as $S(NO) = C(NO)/(C(NO) + 2C(N_2O) + 2C(N_2))$.

3. Results and discussion

3.1. Characterization of perovskite powders and membrane disks

The characterization results of two representative samples used in this study are shown in Table 1. The chemical composition of the materials was determined by XRF and is in excellent agreement with the nominal composition. XRD evidenced that all powders prepared consist of single-phase perovskites, as shown in Fig. 3 for $La_{0.8}Sr_{0.2}FeO_{3-\delta}$ and $La_{0.9}Ca_{0.1}FeO_{3-\delta}$. All the diffraction lines match those of the reference lanthanum iron perovskite ($LaFeO_3$, JCPDS 37–1493). As expected, textural

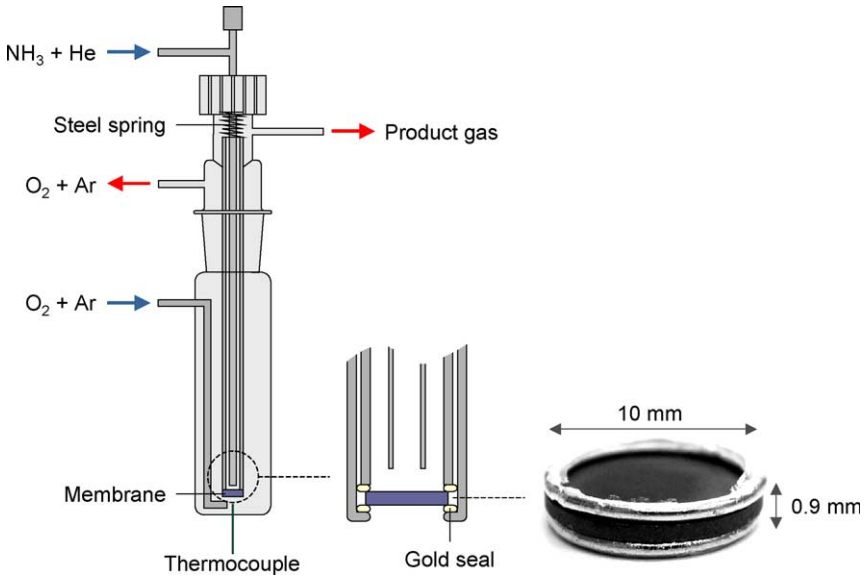

Fig. 2. Quartz reactor used in the membrane tests and photograph of a perovskite membrane disk with the gold seals as obtained after testing.

characterization by N_2 adsorption and Hg porosimetry evidences the low surface area and pore volume of the samples. The absolute (bulk) density of the solids as measured by He pycnometry was ca. 6.4 g cm^{-3}, while the envelope density (including pores and cavities in the solid) was ca. 3.8 g cm^{-3}. The total porosity of the sample (~40%) mainly comes from interparticle voidage. The particle size distribution of the powders previous to the disk fabrication was in the range of 0.1–0.5 μm.

The XRF and XRD results of the membranes lead to no significant changes with respect to the powder precursors (not shown). Fig. 4 shows a SEM micrograph of the surface of the $La_{0.8}Sr_{0.2}FeO_{3-\delta}$ disk. Mapping analyses indicate a homogeneous distribution of elements, as concluded from the uniform colors corresponding to the La, Sr, Fe, and O

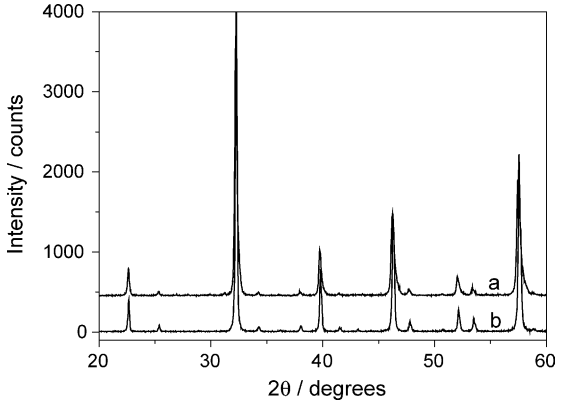

Fig. 3. Powder X-ray diffraction patterns of: (a) $La_{0.8}Sr_{0.2}FeO_{3-\delta}$ and (b) $La_{0.9}Ca_{0.1}FeO_{3-\delta}$.

Table 1
Characterization data of two calcined perovskite powders used in this study

Technique	Characteristic	$La_{0.8}Sr_{0.2}FeO_3$	$La_{0.9}Ca_{0.1}FeO_3$
XRF	Composition (wt.%)	La_2O_3 = 55.3 SrO_3 = 8.4 Fe_2O_3 = 35.4	La_2O_3 = 62.9 CaO = 2.6 Fe_2O_3 = 33.2
	Molar ratio	La/Fe = 0.82 Sr/Fe = 0.19	La/Fe = 0.92 Ca/Fe = 0.11
N_2 adsorption	V_{pore} (cm^3 g^{-1}) S_{BET} (m^2 g^{-1})	0.0089 2.7	0.0046 1.7
Hg porosimetry	V_{pore} (cm^3 g^{-1}) S (m^2 g^{-1}) $\bar{r}_{pore}$ (μm) Porosity (%)	0.11 2.5 0.1 41	0.098 1.6 0.1 37
He pycnometry	$\rho_{absolute}$ (g cm^{-3})	6.46	6.40
Envelope density analysis	$\rho_{envelope}$ (g cm^{-3}) Porosity (%)	3.85 40	3.75 41
Laser diffraction	Particle size (μm)	0.1–0.5	0.1–0.5

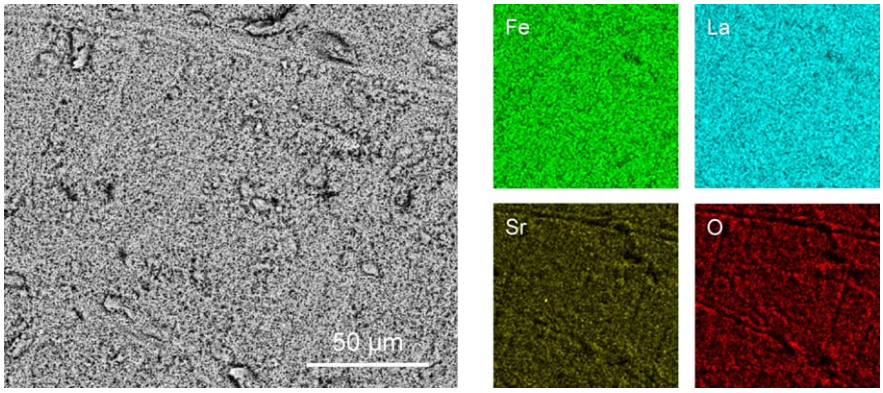

Fig. 4. SEM-EDS analysis of the surface of the $La_{0.8}Sr_{0.2}FeO_{3-\delta}$ membrane disk.

concentrations determined by EDS. Additionally, line analyses were carried out. In these, the metal content is measured along the thickness of the disks in carefully polished sections. Fig. 5 evidences the remarkably constant content of the various metal elements in different points from the membrane surface down to a depth of 30 μm. The values obtained from SEM-EDS are in good agreement with the XRF results (dashed lines in Fig. 5). It should be underlined that the reproducibility of the SEM-EDS results

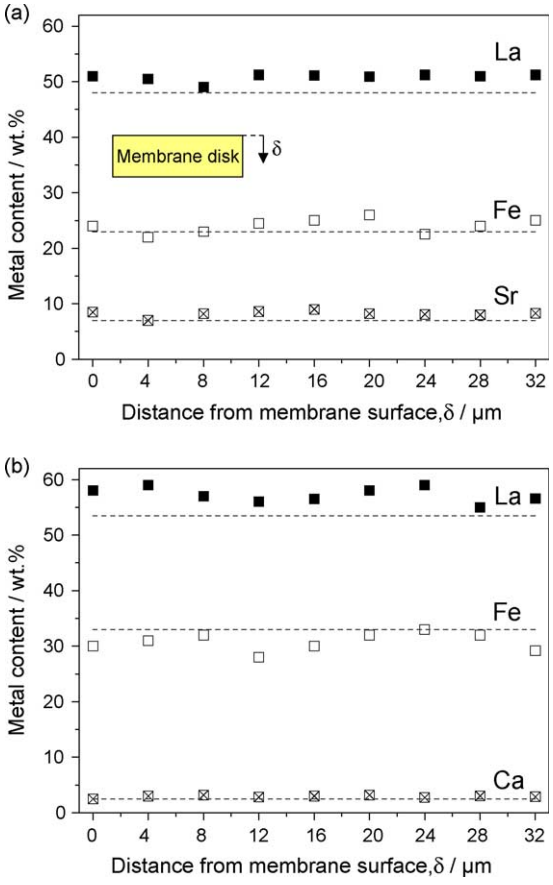

Fig. 5. Line analysis of polished sections of the membrane disks: (a) $La_{0.8}Sr_{0.2}FeO_{3-\delta}$ and (b) $La_{0.9}Ca_{0.1}FeO_{3-\delta}$. Dashed lines represent the content of each element as obtained by XRF.

was confirmed by application of the above procedures in at least three randomly selected spots and sections of the specimens.

3.2. Performance of membrane disks

Important features of perovskite membranes in ammonia oxidation include oxygen flux ($J(O_2)$), selectivity to NO (S(NO)), and chemical stability in reducing and oxidizing atmosphere at high temperature. These interrelated parameters can be tailored by tuning the degree of calcium and strontium substitution in lanthanum ferrite-based perovskites ($La_{1-x}(Sr,Ca)_xFeO_{3-\delta}$). A higher substitution level (x) increases the number of oxygen vacancies (δ) and thus the oxygen flux, but at the expense of lower chemical stability [6,8,9]. Besides, La-substitution by alkaline-earth cations in the perovskite structure is also known to influence the catalytic properties of these mixed oxides [4]. In general terms, this can be caused by variation in the charge and/or coordination of 3d cations, change of the surface chemical composition, and development of micro-heterogeneities at the catalyst surface.

Fig. 6 shows the dependence of the selectivity to nitric oxide and oxygen flux on the inlet ammonia flow at different temperatures over the $La_{0.8}Sr_{0.2}FeO_{3-\delta}$ membrane. Similar curves and dependencies were observed in the other membranes tested. Stable membrane performance over the typical testing period (10 days) was verified by periodically repeating measurements at selected temperature/flow conditions. In the temperature range of 1000–1333 K, NO selectivities in the range of 90–100% can be attained by properly selecting the inlet NH_3 flow. No N_2O was formed in these experiments (<10 ppm), N_2 being the only N-containing by-product. The inlet ammonia flow represented in this and subsequent illustrations is equivalent to the feed ammonia concentration, since the total inlet flow of the NH_3 + He mixture was kept constant (see Section 2). The conversion of ammonia in the experiment was in the relatively narrow range of 82–90%, increasing with temperature and decreasing with increasing the inlet ammonia flow (Fig. 7). The oxygen flux is expected to

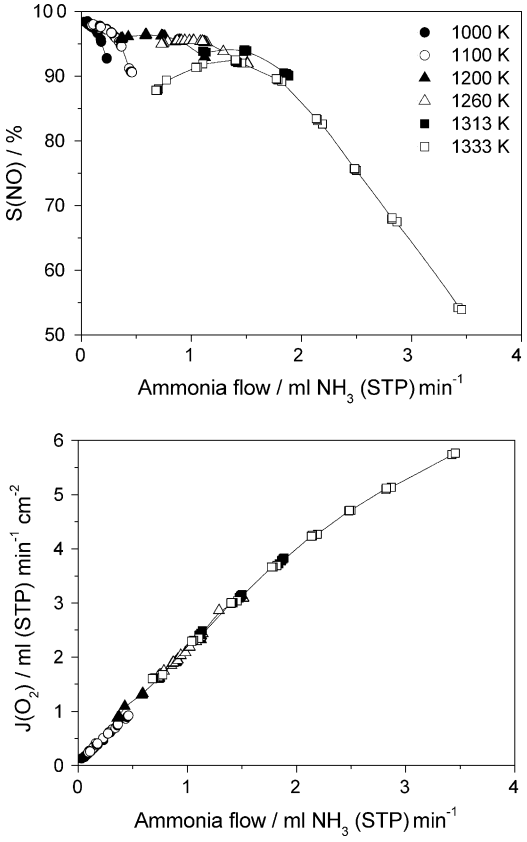

Fig. 6. NO selectivity and O_2 flux vs. inlet ammonia flow during NH_3 oxidation over $La_{0.8}Sr_{0.2}FeO_{3-\delta}$ membrane at different temperatures.

increase with temperature at a fixed oxygen potential gradient. Within our experimental conditions, however, the oxygen flux is controlled by the ammonia flow rate following a linear dependency and is practically unaffected by temperature (Fig. 6). Oxygen fluxes in the range of 0–6 ml O_2 (STP) $min^{-1}\,cm^{-2}$ were obtained over the $La_{0.8}Sr_{0.2}FeO_{3-\delta}$ membrane at the different conditions applied.

Fig. 8 represents the oxygen utilization for ammonia oxidation at the permeate side of the catalytic membrane as

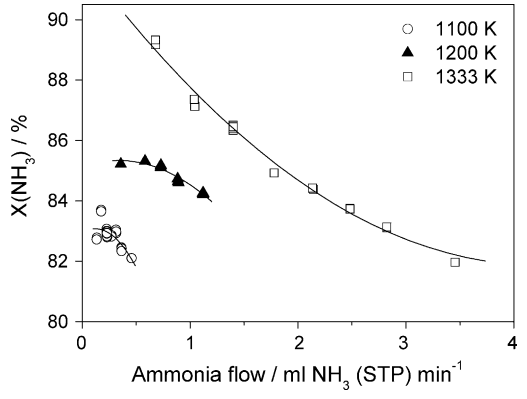

Fig. 7. NH_3 conversion vs. inlet ammonia flow during NH_3 oxidation over $La_{0.8}Sr_{0.2}FeO_{3-\delta}$ membrane at different temperatures.

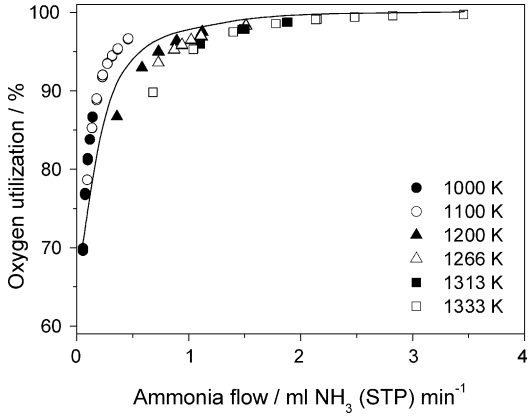

Fig. 8. Oxygen utilization vs. inlet ammonia flow during NH_3 oxidation over $La_{0.8}Sr_{0.2}FeO_{3-\delta}$ membrane at different temperatures.

a function of the ammonia flow at the temperatures investigated. This parameter is defined as:

$$\text{Oxygen utilization} = \left(\frac{C(O_{total}) - 2C(O_2)}{C(O_{total})}\right)$$

where $C(O_{total})$ is the total concentration of oxygen atoms in all O-containing species in the permeate and $C(O_2)$ is the partial oxygen pressure in the product gas. A relatively low oxygen utilization of 70% is obtained at the lowest temperature and inlet ammonia flow applied in our experiments. In other words, at this condition, 30% of the ionic oxygen reaching the surface of the membrane at the permeate side recombines and desorbs as O_2. The catalytic membrane approaches an oxygen utilization of 100% (all oxygen atoms reaching the perovskite surface react with ammonia) when the temperature and/or the inlet flow of NH_3 are increased.

The NO selectivity in Fig. 6 reveals a dependence on temperature, and moreover exhibits a maximum with the inlet ammonia flow. For example, the experiment at 1333 K shows a maximum NO selectivity of ca. 92% at 1.5 ml NH_3 (STP) min^{-1}, corresponding to a feed concentration of 1.1 vol.% NH_3 in He. The NO selectivity sharply decreases at higher NH_3 flows, with a value of 54% at 4.5 ml NH_3 (STP) min^{-1}. Lower ammonia flows also lead to a decreased NO selectivity, e.g. 87% at 0.7 ml NH_3 (STP) min^{-1}. The shift of the NO selectivity maximum to lower ammonia molar flow with decreasing temperature reflects the reduced oxygen flux (at constant oxygen potential) at lower temperatures.

As expected, the NO selectivity decreases in favour of N_2 upon increasing the feed concentration of ammonia due to a favoured recombination of adsorbed NH_x fragments and secondary reactions of NH_x intermediates with NO formed [4]. Fig. 9 displays the ratio of $O_{reacted}/N_{reacted}$ (determined from the oxygen and nitrogen mass balances) versus the inlet ammonia flow. The experiment at 1333 K is particularly illustrative, since a broad range of feed NH_3 concentrations was investigated, leading to a marked NO selectivity

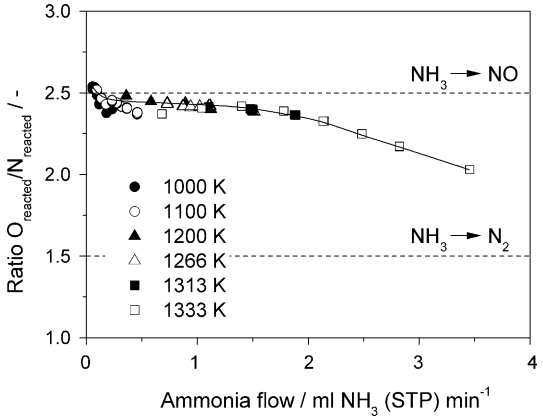

Fig. 9. Ratio of concentrations of atomic oxygen and nitrogen reacted ($O_{reacted}/N_{reacted}$) vs. inlet ammonia flow during NH_3 oxidation over $La_{0.8}Sr_{0.2}FeO_{3-\delta}$ membrane at different temperatures. The dashed lines represent the stoichiometric O/N ratios for ammonia oxidation to nitric oxide (2.5) and nitrogen (1.5).

decreased above 1.5 ml NH_3 (STP) min^{-1} (see Fig. 6). At lower inlet ammonia flows, where NO selectivities in the range of 90% are obtained, the $O_{reacted}/N_{reacted}$ ratio is close from ca. 2.5, in good agreement with the stoichiometry of the ammonia oxidation leading to nitric oxide (see reaction at the permeate side in Fig. 1). At higher ammonia flows, the NO selectivity drops and so does the ratio of $O_{reacted}/N_{reacted}$, resulting in a higher selectivity towards N_2. The gradual trend of a decreased $O_{reacted}/N_{reacted}$ ratio from 2.5 (theoretical NO selectivity of 100%) upon increasing the inlet ammonia flow can be nicely concluded from the plot at all temperatures in Fig. 9.

The slightly decreased NO selectivity at low inlet ammonia flows in Fig. 6 is attributed to secondary reactions occurring in the hot walls of the quartz reactor outlet. This includes the partial oxidation of NH_3 with excess oxygen recombining and escaping the membrane (see Fig. 8) as well as the selective reduction of NO produced with unreacted NH_3. These processes in hot reactor walls downstream the membrane may also explain the decrease in the maximum NO selectivity when going from 1000 K (98%) to 1333 K (92%). Implicitly, with these membrane materials, higher NO selectivities than those displayed in Fig. 6 would have been obtained if post-membrane reactions could have been excluded. Minimizing these involves modifications of the reactor design in Fig. 2, with a rapid quenching of the gas at the membrane outlet.

Fig. 10 shows the maximum NO selectivity and corresponding oxygen flux as functions of the substitution level of Ca and Sr in the lanthanum ferrite perovskites at 1200 K. As expected, the oxygen flux is proportional to the substitution level. The maximum NO selectivity (95–96%) does not depend on the type and degree of substitution within this range, indicating similar catalytic performance of these membrane compositions. Wu et al. [7] studied NH_3 oxidation at 1073 K in a fixed-bed reactor with catalyst particles and reported optimal NO selectivities (ca. 95%) for

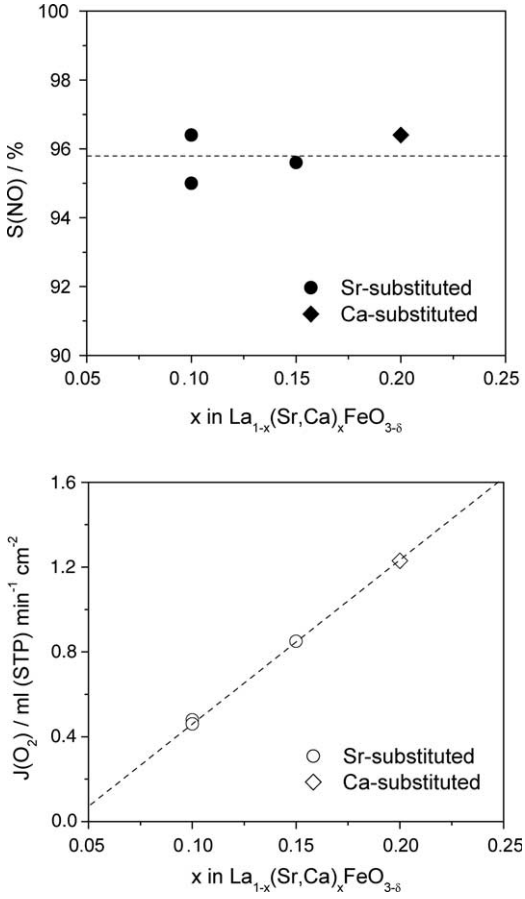

Fig. 10. Maximum NO selectivity and corresponding oxygen flux at 1200 K vs. the substitution level in Ca- and Sr-substituted lanthanum ferrite perovskites.

$x = 0.2$–0.7 in $La_{1-x}Sr_xFeO_3$. For the membrane reactor described here, the optimum substitution level is determined by the combination of maximum flux with absolute chemical stability under process conditions. This optimum substitution level of Sr and Ca probably lie in the range of $x = 0.1$–0.2.

3.3. Membrane-based ammonia oxidation process

Our laboratory results with disks demonstrate the potential of Ca and Sr-substituted lanthanum ferrite membranes for the high-temperature oxidation of ammonia, leading to NO selectivities up to 98%, comparable to the state-of-the-art Pt–Rh alloy gauzes currently installed in industrial ammonia burners [1,2]. In addition, formation of undesirable N_2O is totally suppressed. The implementation of an ammonia oxidation process based on oxygen-conducting membranes will constitute a step change in the production of nitric acid (a top-10 product in the bulk industry), strongly impacting the fertilizer industry. Apart from the superior NO selectivity, in situ O_2 separation from air by application of mixed conducting membranes enables extremely compact and intensified production units, since N_2 represents ca. 70% of the total flow in a current plant. The

lower total flow would allow a drastic size reduction of key units of plants, including the absorption tower and the tail-gas train, as well as the obvious intensification in piping. Moreover, energy savings in compression of the NO_x gas before the absorption step, which requires high pressure, further contributes to more efficient and compact nitric acid plants.

At this stage, it is clear the catalytic membrane configuration introduced in this manuscript is not an alternative to conventional ammonia burners for large-scale nitric acid production. On the other hand, we strongly believe that the membrane concept is particularly attractive for on-site nitric acid production, i.e. decentralized from large existing plants. Our current research focuses on the exploration of modified membrane formulations and materials with an improved oxygen flux in the low-temperature range as compared to the lanthanum ferrites presented here, while keeping the high NO selectivity and zero N_2O emission. In this manner, the feed ammonia concentration at the permeate side of the membrane can be increased, ultimately leading to higher nitric acid capacities. Upon having succeeded on that, scale up of the membrane disks will be decisive for further implementation of the membrane technology in ammonia oxidation. For screening tests in the laboratory, the disk configuration employed is very suitable due to an easy fabrication by a conventional pressing method. However, adopting a multiple planar stack to enlarge the membrane area in industrial scale will originate serious difficulties related to high-temperature sealing and pressure resistance [10]. Tubular membranes have been proposed to reduce problems associated with the high temperature sealing [11], but their small surface area to volume ratio and their relative thick wall (leading to a low oxygen permeation) make them unfavorable in practice. Nonetheless, recently developed hollow fiber membranes possess a much larger membrane area per unit volume for oxygen permeation and a lower resistance due to the thin wall [12–14]. The most elegant and compact reactor configuration clearly involves the application of monolithic membranes. Monoliths possess specific surface areas in the broad range of 500–4000 m^2/m^3 of reactor, depending on cell size and wall thickness [15]. It can be foreseen a reactor design involving the distribution of ammonia and air in the monolithic membrane with square channels according to a chess-board pattern (one channel for ammonia and the four surrounding channels for air). In an ideal situation, a very thin layer of perovskite membrane should be uniformly deposited along selected channels of the extruded monolithic support of the same material as the membrane but with porous walls. It is envisaged that the uniform distribution of the ammonia flow along the channel is a major technical challenge, requiring a precise engineering solution.

4. Conclusions

A greatly intensified manufacture of nitric acid can be achieved by oxidation of ammonia using calcium and strontium-substituted lanthanum ferrite perovskite membranes, originating NO selectivities of 98% in the temperature range of 1000–1333 K. In this process, N_2 is excluded by the oxygen-conducting membranes, expensive noble metal catalysts are unnecessary, and no environmentally harmful N_2O is produced. The membrane-based reactor evidences the great potential for intensification of nitric acid manufacture into a more efficient, compact, and sustainable process, and is considered to be particularly attractive for decentralized production of this important chemical.

References

[1] E. Wagner, T. Fetzer, in: G. Ertl, H. Knözinger, J. Weitkamp (Eds.), Handbook of Heterogeneous Catalysis, vol. 4, VCH, Weinheim, 1997, pp. 1748–1761.
[2] R.J. Farrauto, C.H. Bartholomew, Fundamentals of Industrial Catalytic Processes, Chapman & Hall, London, 1997 , p. 481.
[3] J. Pérez-Ramírez, F. Kapteijn, K. Schöffel, J.A. Moulijn, Appl. Catal. B 44 (2003) 117.
[4] V.A. Sadykov, L.A. Isupova, I.A. Zolotarskii, L.N. Bobrova, A.S. Noskov, V.N. Parmon, E.A. Brushtein, T.V. Telyatnikova, V.I. Chernyshev, V.V. Lunin, Appl. Catal. A 204 (2000) 59 (and references therein).
[5] A. Thursfield, I.S. Metcalfe, J. Mater. Chem. 14 (2004) 2475.
[6] Y. Teraoka, H. Zhang, S. Furukawa, N. Yamazoe, Chem. Lett. (1985) 1743.
[7] Y. Wu, T. Yu, B. Dou, C. Wang, X. Xie, Z. Yu, S. Fan, Z. Fan, L. Wang, J. Catal. 120 (1989) 88.
[8] J.E. ten Elshof, H.J.M. Bouwmeester, H. Verweij, Solid State Ionics 89 (1996) 81.
[9] Y. Takeda, K. Kajiura, S. Naka, M. Takano, in: H. Watanabe, S. Iida, M. Sugimoto (Eds.), Proceedings of the Third International Conference on Ferrites, Japan, 1982, p. 414.
[10] P.N. Dyer, R.E. Richards, S.L. Russek, D.M. Taylor, Solid State Ionics 134 (2000) 21.
[11] H.H. Wang, Y. Cong, W.S. Wang, J. Membr. Sci. 210 (2002) 259.
[12] S. Liu, X. Tan, K. Li, R. Hughes, J. Membr. Sci. 193 (2001) 249.
[13] S. Liu, K. Li, R. Hughes, Mater. Res. Bull. 39 (2004) 119.
[14] J. Luyten, A. Buekenhoudt, W. Adriansens, J. Cooymans, H. Weyten, F. Servaes, R. Leysen, Solid State Ionics 135 (2000) 637.
[15] F. Kapteijn, J.J. Heiszwolf, T.A. Nijhuis, J.A. Moulijn, Cattech 3 (1999) 24.